

Supplement of Biogeosciences, 15, 5395–5413, 2018
<https://doi.org/10.5194/bg-15-5395-2018-supplement>
© Author(s) 2018. This work is distributed under
the Creative Commons Attribution 4.0 License.



Supplement of

Synthetic ozone deposition and stomatal uptake at flux tower sites

Jason A. Ducker et al.

Correspondence to: Jason A. Ducker (jad10d@my.fsu.edu)

The copyright of individual parts of the supplement might differ from the CC BY 4.0 License.

1 S1 Calculation of stomatal conductance and deposition velocity

2
3 Several methods for calculating stomatal conductance and O₃ deposition velocity from eddy
4 covariance measurements are found in literature (e.g. Wesely and Hicks, 1977; Gerosa et al.,
5 2005; Fares et al., 2010). While we follow the same general approach, we present the methods
6 here for completeness and to point out some particular choices we have made. These expressions
7 are used in Eqs. 1-3. The required input variables are O₃ mole fraction (mol mol⁻¹), temperature
8 (K), pressure (Pa), specific humidity (kg kg⁻¹), friction velocity (m s⁻¹), sensible and latent heat
9 fluxes (W m⁻²), canopy height (m), and leaf area index (m² m⁻²).

10
11 The aerodynamic and quasi-laminar layer resistances are calculated from measurements of
12 momentum flux using the Monin-Obukhov similarity relations. For heat, O₃, and other gases, the
13 aerodynamic resistance (r_a , s m⁻¹) is (Foken, 2017, pp. 219-223)

$$14 \quad r_a = \frac{1}{ku_*} \left[\ln \left(\frac{z-d}{z_0} \right) - \psi_H \left(\frac{z-d}{L} \right) + \psi_H \left(\frac{z_0}{L} \right) \right] \quad (A1)$$

15 where r_a is evaluated at height z , u_* is the friction velocity, z_0 (m) is the roughness length for
16 momentum, d (m) is the displacement height, $k = 0.4$ is the von Karman constant, $\psi_H(\zeta)$ is the
17 stability function for sensible heat discussed below, and L is the Obukhov length (m). The
18 roughness and displacement heights are $z_0 = 0.1z_c$ and $d = 0.7z_c$, respectively, where z_c is the
19 canopy height specific to each site (<http://fluxnet.fluxdata.org/sites/site-summary/>, accessed 24
20 February 2017). Since canopy heights are not specified for croplands or grasslands in this
21 database, we use a constant canopy height of 1 m for grasslands and typical crop-specific heights
22 for each agricultural site (Weaver and Bruner, 1927). The stability function is (Foken, 2017, pp.
23 54-62; Högström, 1988)

$$24 \quad \psi_H(\zeta) = \begin{cases} 2 \ln \left(\frac{1 + 0.95(1 - 11.6\zeta)^{1/2}}{2} \right) & \text{for } \zeta < 0 \\ 1 - \left(1 + \frac{2}{3}\zeta \right)^{\frac{3}{2}} - b_1 \left(\zeta - \frac{b_2}{b_3} \right) \exp(-b_3\zeta) - \frac{b_1 b_2}{b_3} & \text{for } \zeta \geq 0 \end{cases} \quad (A2)$$

25 where $b_1 = 0.667$, $b_2 = 5$, and $b_3 = 0.35$. The form above is appropriate for strongly stable
26 conditions ($(z-d)/L = \zeta > 1$), which occur frequently in the FLUXNET2015 data, as well
27 weak stability (Beljaars and Holtslag, 1991).

28
29 The Obukhov length is (Foken, 2017, pp. 54-62)

$$30 \quad L = - \frac{u_*^3 \theta_v}{kg(\overline{w'\theta'_v})} \quad (A3)$$

31 where θ_v is virtual potential temperature, $\overline{w'\theta'_v}$ is the vertical flux of virtual potential temperature
32 or buoyancy at the surface, and g is acceleration due to gravity. For calculations, we expand θ_v
33 and $\overline{w'\theta'_v}$ in terms of measured quantities so

34
$$L = - \frac{u_*^3 c_p \rho \theta (1 + 0.61q)}{kg(H(1 + 0.61q) + 0.61c_p \theta E)} \quad (\text{A4})$$

35 where c_p is specific heat capacity of air ($\text{J kg}^{-1} \text{K}^{-1}$), ρ is the mass density of air (kg m^{-3}), θ is
 36 potential temperature (K), q is specific humidity (kg kg^{-1}), H is the surface sensible heat flux (W
 37 m^{-2}), and E is the surface moisture flux ($\text{kg m}^{-2} \text{s}^{-1}$). H and E are defined positive for upward
 38 fluxes.

39
 40 The quasi-laminar layer resistance for O_3 and H_2O is (Foken, 2017, pp. 219-223)

41
$$r_b = \frac{2}{ku_*} \left(\frac{\text{Sc}}{\text{Pr}} \right)^{2/3}, \quad (\text{A5})$$

42 where $\text{Sc} = \nu/D$ is the Schmidt number, which is the ratio of kinematic viscosity of air (ν) to the
 43 molecular diffusivity of the gas in air (D), and $\text{Pr} = \nu/D_H$ is the Prandtl number, which involves
 44 the thermal diffusivity (D_H). The conductance for heat is the same as Eq. A5, but uses the
 45 thermal diffusivity of air in place of molecular diffusivity.

46
 47 We calculate stomatal resistance and conductance from the evaporative-resistance form of the
 48 Penman-Monteith equation (Monteith, 1981; Gerosa et al., 2007). For water vapor,

49
$$g_{s,w}^{-1} = r_{s,w} = \frac{\varepsilon \rho (e_s(T_f) - e)}{pE} - (r_a + r_{b,w}) \quad (\text{A6})$$

50 where $\varepsilon = 0.622$ is the mass ratio of H_2O and dry air, p is the air pressure, $e_s(T_f)$ is the saturation
 51 vapor pressure at the transpiring leaf surface with temperature T_f , e is vapor pressure at the flux
 52 measurement height, and $r_{b,w}$ is the quasi-laminar layer resistance to water vapor (Eq. A5). Leaf
 53 temperature is not a standard FLUXNET2015 variable, but it can be estimated from sensible heat
 54 flux using surface energy balance (Gerosa et al., 2007):

55
$$T_f = T + \frac{H}{c_p \rho} (r_a + r_{b,H}) \quad (\text{A7})$$

56 where T is the air temperature at the measurement height and $r_{b,H}$ is the quasi-laminar layer
 57 resistance to heat (Eq. A5). We initially inverted Monteith's (1981) original equation for
 58 evapotranspiration (Eq. 4 in Gerosa et al., 2007) in place of Eq. A6, but the resulting $g_{s,w}$
 59 estimates were much more noisy. Although the forms are analytically equivalent (Gerosa et al.,
 60 2007), inverting the evaporative-resistance form is numerically preferable because it avoids
 61 subtractive terms that amplify relative errors and it more accurately treats temperature and
 62 pressure effects, particularly the non-linearity in the saturation vapor pressure.

63
 64 The stomatal conductance of O_3 is less than water vapor due to its greater molar mass and
 65 diffusion against the net gas flow out of the stomatal pore (Marrero and Mason, 1972), so

66
$$g_s = 0.6 g_{s,w}. \quad (\text{A8})$$

67 In all equations, we include the temperature and pressure dependences of ρ , c_p , v , D , D_H , and
 68 latent heat of vaporization and also the humidity dependence of ρ , c_p , and D_H using expressions
 69 from Jacobson (2005).

70
 71

72 **S2 Propagation of uncertainty**

73

74 We estimate uncertainties in all derived quantities using standard techniques for propagation of
 75 errors (e.g. Taylor, 1997, pp. 73-77). In the following section, f is a function that depends on
 76 variables x_1, x_2, \dots, x_n that each have uncertainties $\sigma_{x_1}, \sigma_{x_2}, \dots, \sigma_{x_n}$. The standard error (σ_f) in
 77 $f(x_1, x_2, \dots, x_n)$ at time i is approximately

$$78 \quad \sigma_{f,i}^2 = \sum_{j=1}^n \left(\frac{\partial f_i}{\partial x_j} \right)^2 \sigma_{x_j,i}^2. \quad (\text{B1})$$

79 This form neglects covariance between the measurement errors, which is unknown in our case,
 80 and is most accurate when $\sigma_{x_j} \ll x_j$. We use centered finite differences to calculate numerical
 81 derivatives through all equations.

82

83 The propagation of errors reveals that F_{s,O_3}^{syn} and other quantities have errors or uncertainties that
 84 vary widely from hour to hour. Daily and monthly averages should account for the varying
 85 confidence in each value in the average (e.g. Taylor, 1997, pp. 173-177). For values f_i that are
 86 from a single distribution, but have different uncertainties $\sigma_{f,i}$, the maximum likelihood estimate
 87 of f is

$$88 \quad \bar{f} = \left(\sum_{i=1}^m w_i f_i \right) \left(\sum_{i=1}^m w_i \right)^{-1}; \quad w_i = \sigma_{f,i}^{-2}. \quad (\text{B2})$$

89 The weights w_i reflect the confidence in value f_i and the summation is carried out over all times
 90 m within the desired averaging period. The standard error of \bar{f} is

$$91 \quad \sigma_{\bar{f}} = \left(\sum_{i=1}^m w_i \right)^{-\frac{1}{2}}. \quad (\text{B3})$$

92 For averaging across times when f is expected to change, as during different hours of the day, an
 93 unweighted average is more appropriate

$$94 \quad \bar{f} = \frac{1}{m} \sum_{i=1}^m f_i \quad (\text{B4})$$

95 and the standard error of \bar{f} , given by Eq. B1, simplifies to

$$96 \quad \sigma_{\bar{f}} = \left(\frac{1}{m^2} \sum_{i=1}^m \sigma_{f,i}^2 \right)^{\frac{1}{2}}. \quad (\text{B5})$$

97 **S3 Stomatal and non-stomatal O₃ deposition at Harvard Forest**

98
99 Our estimate of the non-stomatal fraction of O₃ deposition at Harvard Forest (mean 8%, range –
100 33 to 34%; Sect. 3.2) is smaller than was previously reported at that site (mean 40%, range 20-
101 60%; Clifton et al., 2017). The main reason for the different results is the re-calibration of the
102 water vapor fluxes in this work, which is described in Sect. 2.2. Here, we show how other
103 differences between our analysis and that of Clifton et al. (2017) affect the estimate of non-
104 stomatal fraction of O₃ deposition at Harvard Forest. Using our gap-filled data, the mean
105 estimate of the non-stomatal fraction of O₃ deposition at Harvard Forest does not change but the
106 range slightly increases (8%, range –36 to 38%). With uncorrected water vapor fluxes, our
107 estimate would be 51% (range: 32% to 63%). If we also ignore the propagated uncertainty,
108 which varies from hour to hour, and calculate averages with equal weight (i.e. equal uncertainty)
109 for each time interval, as Clifton et al. did, then we would estimate 53% (range: 34% to 66%). If
110 we also use data filtering criteria from Clifton et al. (i.e. remove 3 σ outliers of v_d and g_s , but no
111 filtering for precipitation and high relative humidity), then we would estimate 48% (range: 28%
112 to 61%). Finally, if we also restrict our averages to 9am-3pm, as Clifton et al. did, instead of all
113 daylight data, then we would estimate 45% (range: 25% to 60%). This final estimate is very
114 close to the method and value reported by Clifton et al. (2017). The remaining small differences
115 are probably due to Clifton et al. including 1992 in their analysis and differences in the form of
116 the Penman-Monteith and stability functions. Since the re-calibration of water vapor fluxes (Sect.
117 2.2) is an improvement in this work and the main reason for our results differing from Clifton et
118 al. (2017), our estimates of small non-stomatal fraction O₃ deposition at Harvard Forest appear to
119 be most reliable estimate for this site.
120

Table S1. Description of FLUXNET2015 Tier 1 sites used in SynFlux.

| Site name | PFT ¹ | Lat ² | Lon ³ | Clim ⁴ | Period | References ⁵ |
|---------------------|------------------|------------------|------------------|-------------------|-----------|--------------------------------|
| AT-Neu | GRA | 47.1167 | 11.3175 | Unk | 2002-2012 | (Wohlfahrt et al., 2008) |
| BE-Bra | MF | 51.3092 | 4.5206 | Unk | 1996-2014 | (Carrara et al., 2004) |
| BE-Lon | CRO | 50.5516 | 4.7461 | Cfb | 2004-2014 | (Moureaux et al., 2006) |
| BE-Vie | MF | 50.3051 | 5.9981 | Cfb | 1996-2014 | (Aubinet et al., 2001) |
| CH-Cha | GRA | 47.2102 | 8.4104 | Unk | 2005-2014 | (Merbold et al., 2014) |
| CH-Dav | ENF | 46.8153 | 9.8559 | Unk | 1997-2014 | (Zielis et al., 2014) |
| CH-Fru | GRA | 47.1158 | 8.5378 | Unk | 2005-2014 | (Imer et al., 2013) |
| CH-Lae | MF | 47.4781 | 8.3650 | Unk | 2004-2014 | (Etzold et al., 2011) |
| CH-Oe1 | GRA | 47.2858 | 7.7319 | Unk | 2002-2008 | (Ammann et al., 2009) |
| CH-Oe2 | CRO | 47.2863 | 7.7343 | Unk | 2004-2014 | (Dietiker et al., 2010) |
| CZ-BK1 | ENF | 49.5021 | 18.5369 | Unk | 2004-2008 | (Acosta et al., 2013) |
| CZ-BK2 | GRA | 49.4944 | 18.5429 | Unk | 2004-2006 | – |
| CZ-wet | WET | 49.0247 | 14.7704 | Unk | 2006-2014 | (Důšek et al., 2012) |
| DE-Akm | WET | 53.8662 | 13.6834 | Cfb | 2009-2014 | – |
| DE-Geb | CRO | 51.1001 | 10.9143 | Unk | 2001-2014 | (Anthoni et al., 2004) |
| DE-Gri | GRA | 50.9500 | 13.5126 | Cfb | 2004-2014 | (Prescher et al., 2010a) |
| DE-Hai | DBF | 51.0792 | 10.4530 | Unk | 2000-2012 | (Knohl et al., 2003) |
| DE-Kli | CRO | 50.8931 | 13.5224 | Cfb | 2004-2014 | (Prescher et al., 2010) |
| DE-Lkb | ENF | 49.0996 | 13.3047 | Unk | 2009-2013 | (Lindauer et al., 2014) |
| DE-Obe | ENF | 50.7867 | 13.7213 | Cfb | 2008-2014 | – |
| DE-RuR ⁶ | GRA | 50.6219 | 6.3041 | Unk | 2011-2014 | (Post et al., 2015) |
| DE-RuS ⁶ | CRO | 50.8659 | 6.4472 | Cfb | 2011-2014 | (Mauder et al., 2013) |
| DE-Seh | CRO | 50.8706 | 6.4497 | Unk | 2007-2010 | (Schmidt et al., 2012) |
| DE-SfN | WET | 47.8064 | 11.3275 | Unk | 2012-2014 | (Hommeltenberg et al., 2014) |
| DE-Spw | WET | 51.8923 | 14.0337 | Cfb | 2010-2014 | – |
| DE-Tha | ENF | 50.9624 | 13.5652 | Cfb | 1996-2014 | (Grünwald and Bernhofer, 2007) |
| DK-Fou | CRO | 56.4842 | 9.5872 | Unk | 2005-2005 | – |
| DK-Sor | DBF | 55.4859 | 11.6446 | Unk | 1996-2014 | (Pilegaard et al., 2011) |
| ES-LgS | OSH | 37.0979 | -2.9658 | Unk | 2007-2009 | (Reverter et al., 2010) |
| ES-Ln2 | OSH | 36.9695 | -3.4758 | Unk | 2009-2009 | – |
| FI-Hyy | ENF | 61.8474 | 24.2948 | Unk | 1996-2014 | (Mammarella et al., 2007) |
| FI-Jok | CRO | 60.8986 | 23.5135 | Unk | 2000-2003 | (Lohila, 2004) |
| FI-Lom | WET | 67.9972 | 24.2092 | Unk | 2007-2009 | – |
| FI-Sod | ENF | 67.3619 | 26.6378 | Unk | 2001-2014 | (Thum et al., 2007) |
| FR-Fon | DBF | 48.4764 | 2.7801 | Cfb | 2005-2014 | (Delpierre et al., 2015) |
| FR-Gri | CRO | 48.8442 | 1.9519 | Cfb | 2004-2013 | (Loubet et al., 2011) |
| FR-LBr | ENF | 44.7171 | -0.7693 | Unk | 1996-2008 | (Berbigier et al., 2001) |
| FR-Pue | EBF | 43.7414 | 3.5958 | Unk | 2000-2014 | (Rambal et al., 2004) |
| IT-BCi | CRO | 40.5238 | 14.9574 | Unk | 2004-2014 | (Vitale et al., 2015) |
| IT-CA1 | DBF | 42.3804 | 12.0266 | Unk | 2011-2014 | (Sabbatini et al., 2016) |
| IT-CA2 | CRO | 42.3772 | 12.0260 | Unk | 2011-2014 | (Sabbatini et al., 2016) |
| IT-CA3 | DBF | 42.3800 | 12.0222 | Unk | 2011-2014 | (Sabbatini et al., 2016) |
| IT-Col | DBF | 41.8494 | 13.5881 | Unk | 1996-2014 | (Valentini et al., 1996) |

| | | | | | | |
|--------|-----|---------|-----------|-----|-----------|----------------------------|
| IT-Cp2 | EBF | 41.7043 | 12.3573 | Unk | 2012-2014 | (Fares et al., 2014) |
| IT-Cpz | EBF | 41.7052 | 12.3761 | Unk | 1997-2009 | (Garbulsky et al., 2008) |
| IT-Isp | DBF | 45.8126 | 8.6336 | Unk | 2013-2014 | (Ferréa et al., 2012) |
| IT-La2 | ENF | 45.9542 | 11.2853 | Unk | 2000-2002 | (Marcolla et al., 2003) |
| IT-Lav | ENF | 45.9562 | 11.2813 | Unk | 2003-2014 | (Marcolla et al., 2003) |
| IT-MBo | GRA | 46.0147 | 11.0458 | Unk | 2003-2013 | (Marcolla et al., 2011) |
| IT-Noe | CSH | 40.6061 | 8.1515 | Unk | 2004-2014 | (Papale et al., 2014) |
| IT-PT1 | DBF | 45.2009 | 9.0610 | Unk | 2002-2004 | (Migliavacca et al., 2009) |
| IT-Ren | ENF | 46.5869 | 11.4337 | Unk | 1998-2013 | (Montagnani et al., 2009) |
| IT-Ro1 | DBF | 42.4081 | 11.9300 | Unk | 2000-2008 | (Rey et al., 2002) |
| IT-Ro2 | DBF | 42.3903 | 11.9209 | Unk | 2002-2012 | (Tedeschi et al., 2006) |
| IT-SR2 | ENF | 43.7320 | 10.2910 | Unk | 2013-2014 | – |
| IT-SRo | ENF | 43.7279 | 10.2844 | Unk | 1999-2012 | (Chiesi et al., 2005) |
| IT-Tor | GRA | 45.8444 | 7.5781 | Unk | 2008-2014 | (Galvagno et al., 2013) |
| NL-Hor | GRA | 52.2404 | 5.0713 | Unk | 2004-2011 | (Jacobs et al., 2007) |
| NL-Loo | ENF | 52.1666 | 5.7436 | Unk | 1996-2013 | (Dolman et al., 2002) |
| RU-Fyo | ENF | 56.4615 | 32.9221 | Unk | 1998-2014 | (Kurbatova et al., 2008) |
| US-AR1 | GRA | 36.4267 | -99.4200 | Dsa | 2009-2012 | (Raz-Yaseef et al., 2015) |
| US-AR2 | GRA | 36.6358 | -99.5975 | Dsa | 2009-2012 | (Raz-Yaseef et al., 2015) |
| US-ARb | GRA | 35.5497 | -98.0402 | Cfa | 2005-2006 | (Raz-Yaseef et al., 2015) |
| US-ARc | GRA | 35.5465 | -98.0400 | Cfa | 2005-2006 | (Raz-Yaseef et al., 2015) |
| US-ARM | CRO | 36.6058 | -97.4888 | Cfa | 2003-2012 | (Fischer et al., 2007) |
| US-Blo | ENF | 38.8953 | -120.6328 | Csa | 1997-2007 | (Goldstein et al., 2000) |
| US-Cop | GRA | 38.0900 | -109.3900 | Unk | 2001-2007 | (Bowling et al., 2010) |
| US-GBT | ENF | 41.3658 | -106.2397 | Dfc | 1999-2006 | (Zeller and Nikolov, 2000) |
| US-GLE | ENF | 41.3665 | -106.2399 | Dfc | 2004-2014 | (Frank et al., 2014) |
| US-Ha1 | DBF | 42.5378 | -72.1715 | Dfb | 1991-2012 | (Urbanski et al., 2007) |
| US-KS2 | CSH | 28.6086 | -80.6715 | Cwa | 2003-2006 | (Powell et al., 2006) |
| US-Los | WET | 46.0827 | -89.9792 | Dfb | 2000-2014 | (Sulman et al., 2009) |
| US-Me1 | ENF | 44.5794 | -121.5000 | Csb | 2004-2005 | (Irvine et al., 2007) |
| US-Me2 | ENF | 44.4523 | -121.5574 | Csb | 2002-2014 | (Irvine et al., 2008) |
| US-Me6 | ENF | 44.3233 | -121.6078 | Csb | 2010-2014 | (Ruehr et al., 2012) |
| US-MMS | DBF | 39.3232 | -86.4131 | Cfa | 1999-2014 | (Dragoni et al., 2011) |
| US-Myb | WET | 38.0498 | -121.7651 | Csa | 2010-2014 | (Matthes et al., 2014) |
| US-Ne1 | CRO | 41.1651 | -96.4766 | Dfa | 2001-2013 | (Verma et al., 2005) |
| US-Ne2 | CRO | 41.1649 | -96.4701 | Dfa | 2001-2013 | (Verma et al., 2005) |
| US-Ne3 | CRO | 41.1797 | -96.4397 | Dfa | 2001-2013 | (Verma et al., 2005) |
| US-NR1 | ENF | 40.0329 | -105.5464 | Dfc | 1998-2014 | (Monson et al., 2002) |
| US-ORv | WET | 40.0201 | -83.0183 | Cfa | 2011-2011 | (Morin et al., 2014) |
| US-PFa | MF | 45.9459 | -90.2723 | Dfb | 1995-2014 | (Desai et al., 2015) |
| US-SRG | GRA | 31.7894 | -110.8277 | Bsk | 2008-2014 | (Scott et al., 2015) |
| US-SRM | WSA | 31.8214 | -110.8661 | Bsk | 2004-2014 | (Scott et al., 2009) |
| US-Syv | MF | 46.2420 | -89.3477 | Dfb | 2001-2014 | (Desai et al., 2005) |
| US-Ton | WSA | 38.4316 | -120.9660 | Csa | 2001-2014 | (Baldocchi et al., 2010) |
| US-Tw1 | WET | 38.1074 | -121.6469 | Csa | 2012-2014 | (Oikawa et al., 2017) |
| US-Tw2 | CRO | 38.1047 | -121.6433 | Csa | 2012-2013 | (Knox et al., 2016) |

| | | | | | | |
|--------|-----|---------|-----------|-----|-----------|--------------------------|
| US-Tw3 | CRO | 38.1159 | -121.6467 | Csa | 2013-2014 | (Baldocchi et al., 2015) |
| US-Tw4 | WET | 38.1030 | -121.6414 | Csa | 2013-2014 | (Baldocchi, 2016) |
| US-Twt | CRO | 38.1087 | -121.6530 | Csa | 2009-2014 | (Hatala et al., 2012) |
| US-UMB | DBF | 45.5598 | -84.7138 | Dfb | 2000-2014 | (Gough et al., 2013) |
| US-UMd | DBF | 45.5625 | -84.6975 | Dfb | 2007-2014 | (Gough et al., 2013) |
| US-Var | GRA | 38.4133 | -120.9507 | Csa | 2000-2014 | (Ma et al., 2007) |
| US-WCr | DBF | 45.8059 | -90.0799 | Dfb | 1999-2014 | (Cook et al., 2004) |
| US-Whs | OSH | 31.7438 | -110.0522 | Bsk | 2007-2014 | (Scott et al., 2015) |
| US-Wi0 | ENF | 46.6188 | -91.0814 | Dfb | 2002-2002 | (Noormets et al., 2007) |
| US-Wi3 | DBF | 46.6347 | -91.0987 | Dfb | 2002-2004 | (Noormets et al., 2007) |
| US-Wi4 | ENF | 46.7393 | -91.1663 | Dfb | 2002-2005 | (Noormets et al., 2007) |
| US-Wi6 | OSH | 46.6249 | -91.2982 | Dfb | 2002-2003 | (Noormets et al., 2007) |
| US-Wi9 | ENF | 46.6188 | -91.0814 | Dfb | 2004-2005 | (Noormets et al., 2007) |
| US-Wkg | GRA | 31.7365 | -109.9419 | Bsk | 2004-2014 | (Scott et al., 2010) |

123 ¹ Plant functional type; see Table 2 for abbreviations.

124 ² Positive value indicates north latitude.

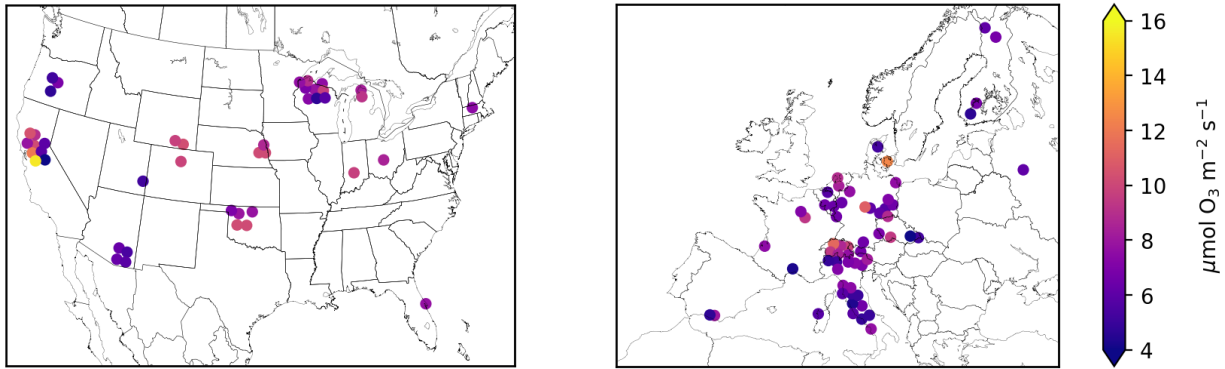
125 ³ Negative value indicates west longitude.

126 ⁴ Köppen Climate classification.

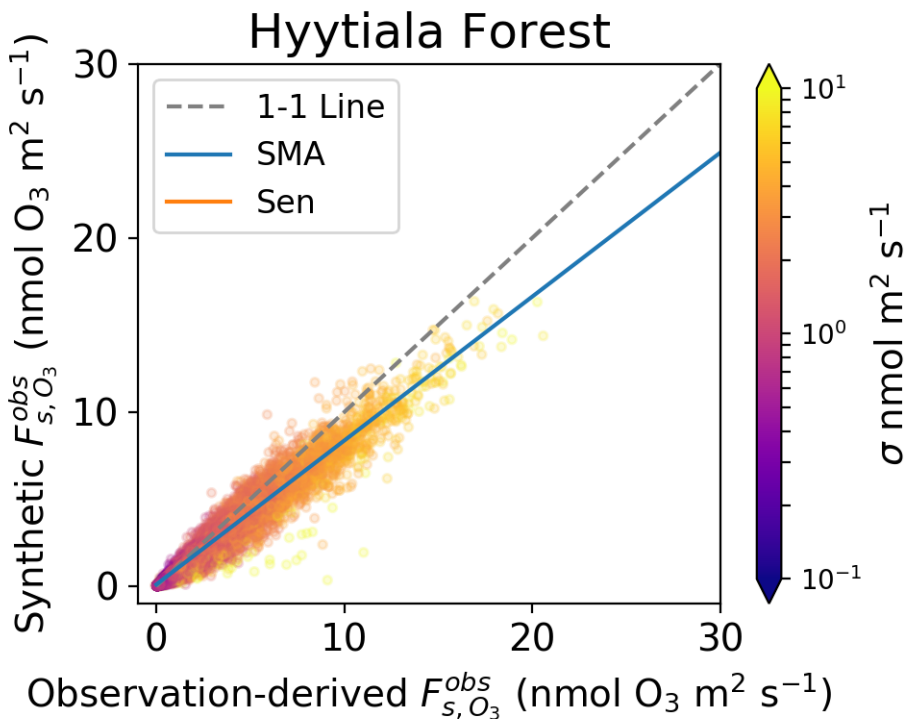
127 ⁵ “-” indicates that site operators have not provided a reference.

128 ⁶ Latent and sensible heat flux uncertainty not reported for this site; 50% uncertainty is
129 assumed.

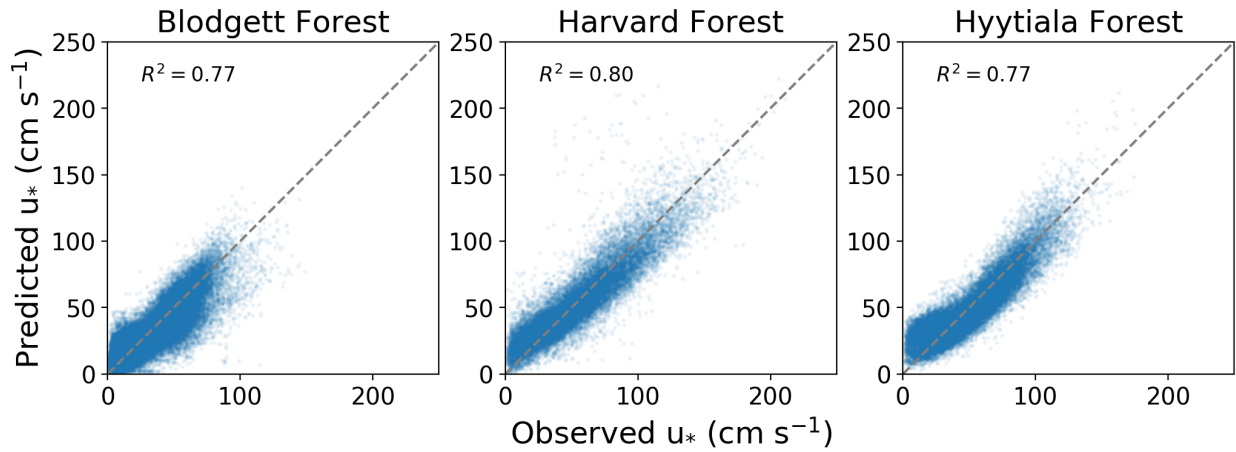
130



131
 132 Figure S1. Mean synthetic total O₃ flux ($F_{O_3}^{syn}$, Sect. 2.1) during the daytime growing season at
 133 FLUXNET2015 sites in the United States and Europe. Symbols of some sites have been moved
 134 slightly to reduce overlap and improve legibility.
 135
 136

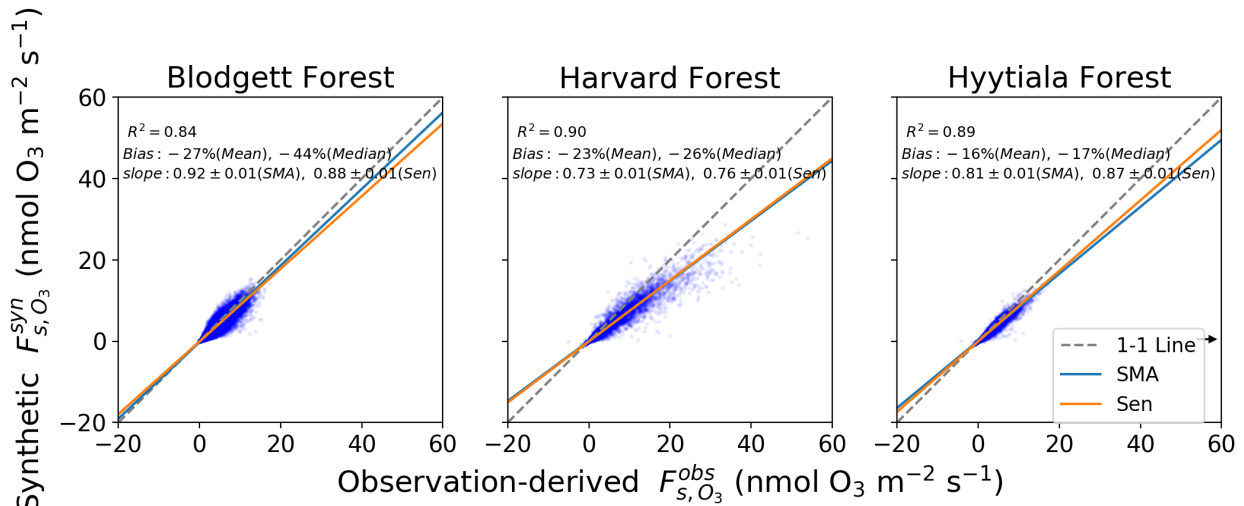


137
 138 Figure S2. Synthetic and observed stomatal conductance, F_{s,O_3}^{syn} , at Hyytiälä Forest illustrating the
 139 errors in half-hourly data. Colors show the standard deviation of each value on a logarithmic
 140 scale, as calculated by error propagation.
 141



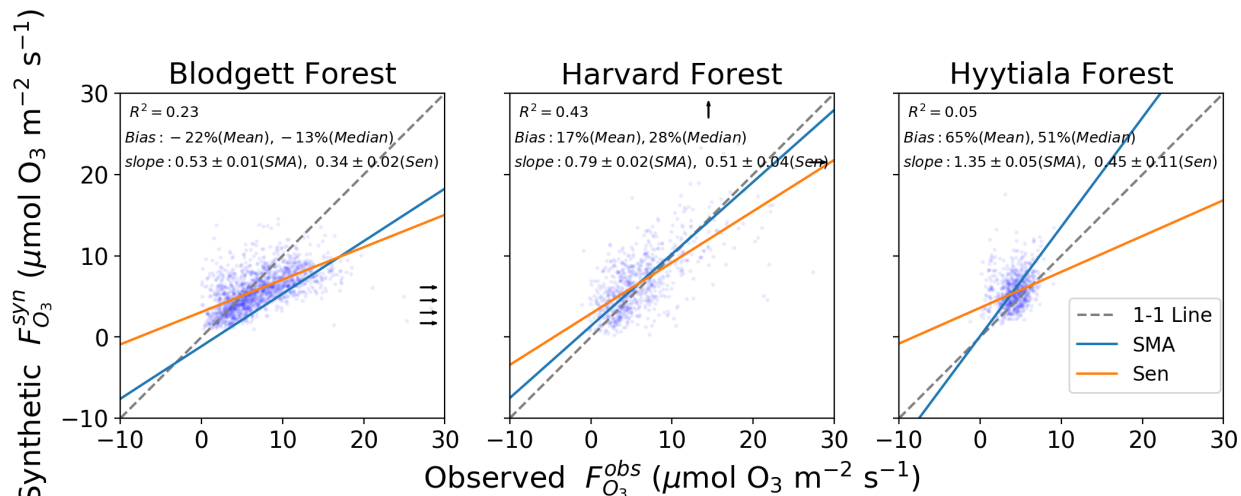
142
143
144
145

Figure S3. Observed and predicted friction velocity (u_*) from the regression model in Sect 2.3.



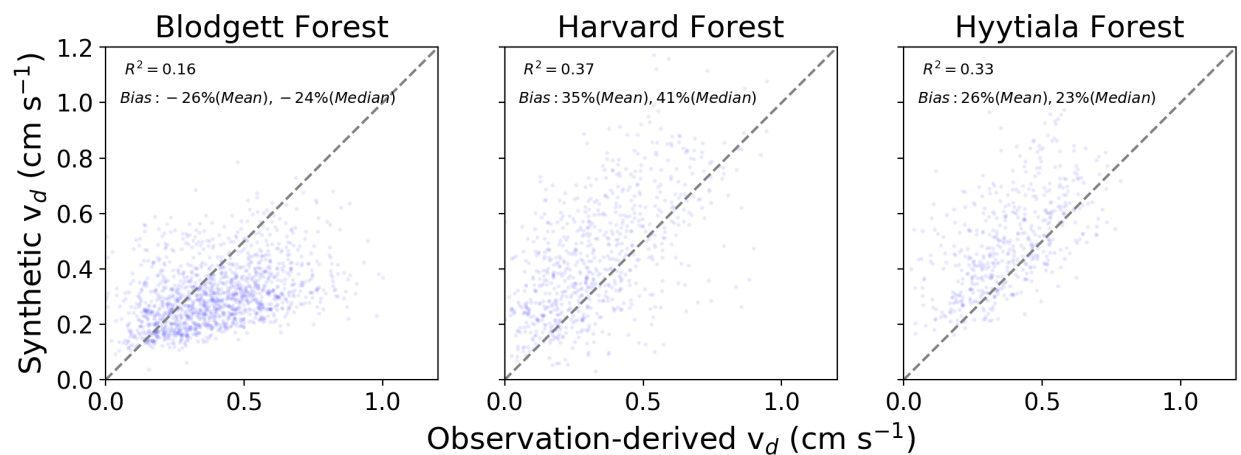
146
147
148
149
150

Figure S4. Synthetic and observation-derived half-hourly (hourly at Harvard Forest) stomatal O_3 flux. See Fig. 2 for explanation of lines and inset text.

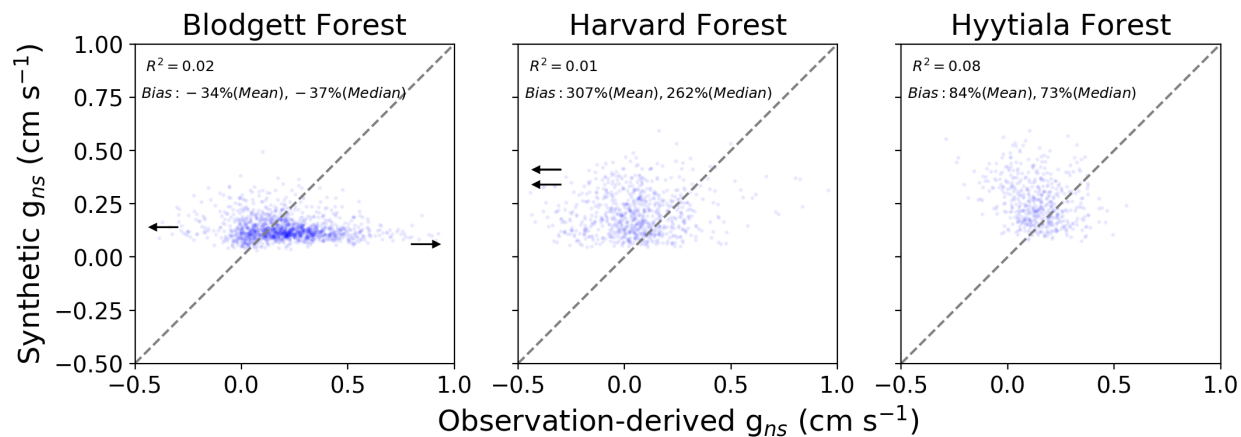


151
 152 Figure S5. Synthetic and observation-derived daily daytime total O_3 flux ($F_{O_3}^{syn}$, Sect. 2.1). See
 153 Sect. 2.1 for explanation of $F_{O_3}^{syn}$ and Fig. 2 for explanation of lines and inset text.

154
 155

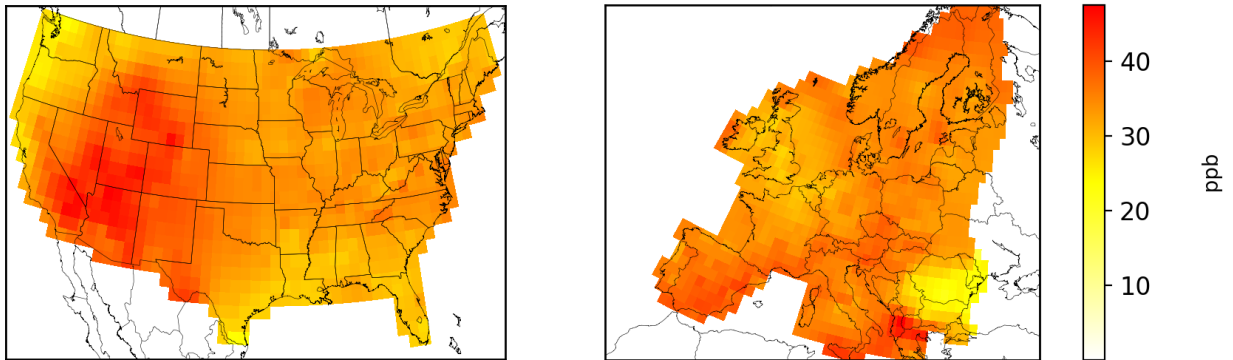


156
 157 Figure S6. Synthetic and observation-derived daily daytime O_3 deposition velocity.
 158



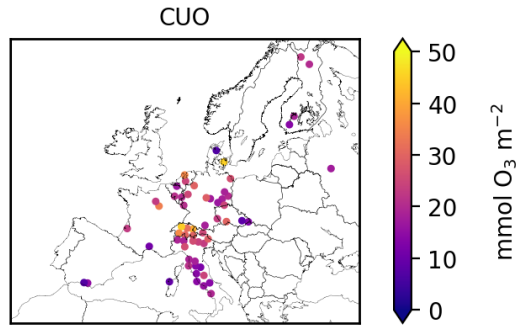
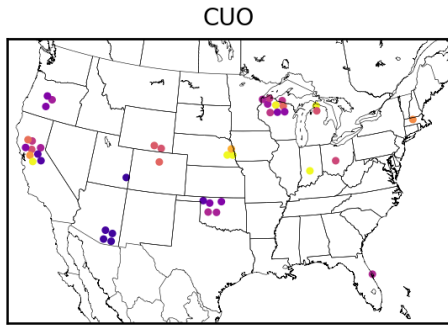
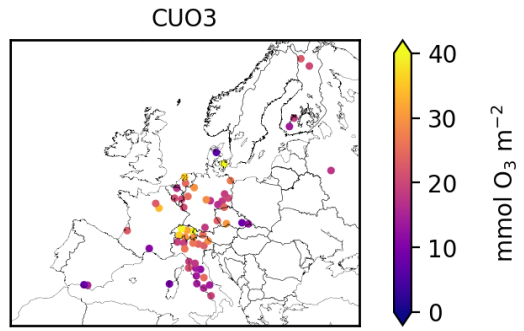
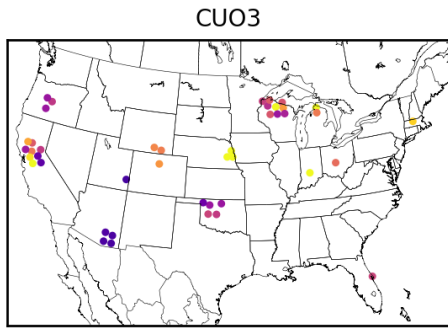
159

160 Figure S7. Synthetic and observation-derived daily daytime O₃ non-stomatal conductance.
161
162
163

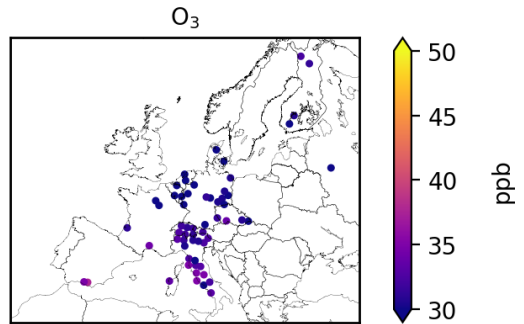
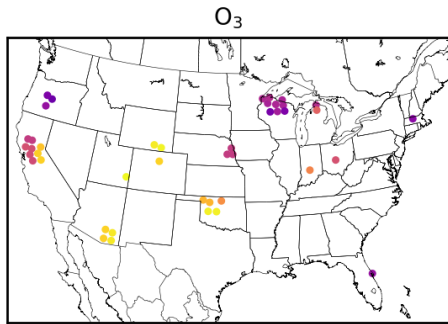


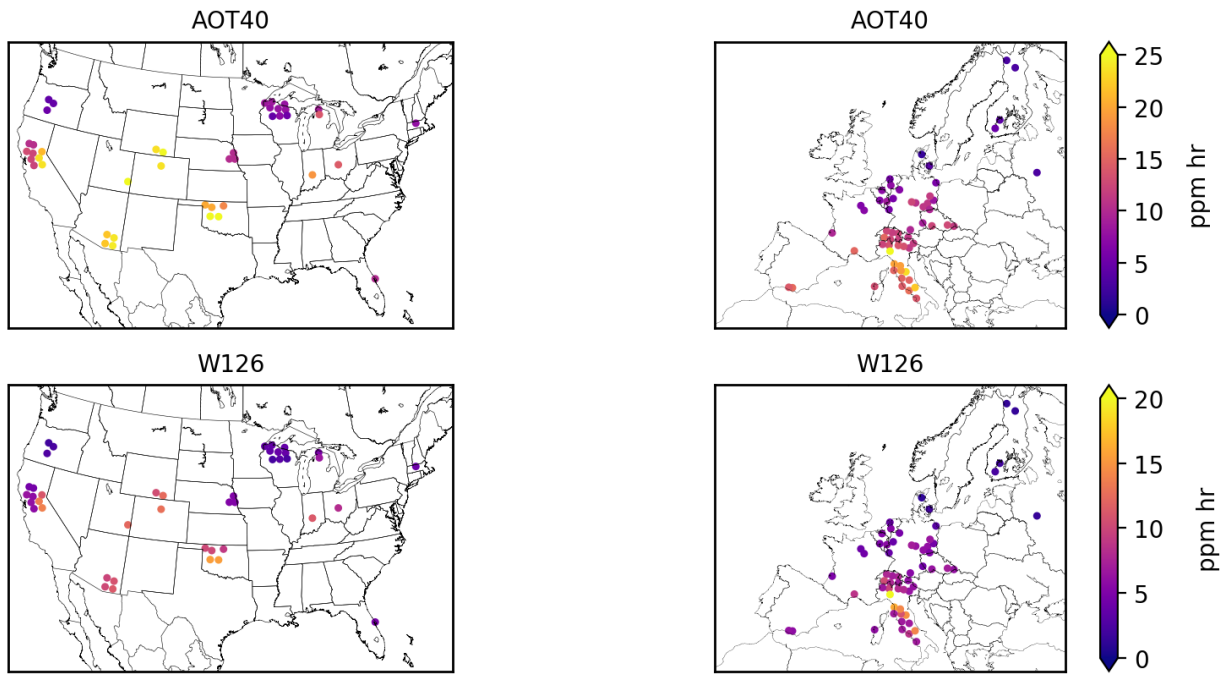
164
165 Figure S8. Mean daytime (8:00am-8:00pm local) O₃ concentrations for the US and Europe
166 during the growing season (typically April-September) for 2000-2014. Data from Schnell et al.
167 (2014).
168

169



170





171
 172 Figure S9. Metrics of plant exposure to O₃ at FLUXNET2015 sites in the US and Europe: CUO₃,
 173 CUO, mean O₃, AOT40, and W126. See Sect. 3.4 for metric definitions.

174
 175